

RUSSIAN ACADEMY OF SCIENCES

NATIONAL GEOPHYSICAL COMMITTEE

РОССИЙСКАЯ АКАДЕМИЯ НАУК

НАЦИОНАЛЬНЫЙ ГЕОФИЗИЧЕСКИЙ КОМИТЕТ



NATIONAL REPORT

for the

International Association of
Seismology and Physics of the Earth's Interior
of the

International Union of Geodesy and Geophysics
2011–2014

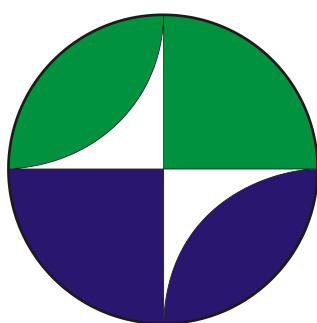
НАЦИОНАЛЬНЫЙ ОТЧЕТ

для

Международной ассоциации
сейсмологии и физики недр Земли

Международного
геодезического и геофизического союза
2011–2014

Москва 2015 Moscow



**Presented to the XXVI General Assembly
of the
International Union of Geodesy and Geophysics**

**К XXVI Генеральной ассамблее
Международного геодезического и геофизического
союза**

RUSSIAN ACADEMY OF SCIENCES

National Geophysical Committee

NATIONAL REPORT

for the

International Association of

Seismology and Physics of the Earth's Interior

of the

International Union of Geodesy and Geophysics

2011–2014

Presented to the XXVI General Assembly

of the

IUGG

2015

Moscow

In this National Report are given major results of researches conducted by Russian geophysicists in 2011–2014 on the topics of the International Association of Seismology and the Physics of the Earth's Interior (IASPEI) of the International Union of Geodesy and Geophysics (IUGG). This report is prepared by the Section of Seismology and Physics of the Earth's Interior of the National Geophysical Committee of Russia.

В данном Национальном отчете представлены основные результаты исследований, проводимых российскими учеными в 2011—2014 гг., по темам, соответствующим направлениям деятельности Международной ассоциации сейсмологии и физики недр Земли (МАСФНЗ) Международного геодезического и геофизического союза (МГГС). Данный отчет подготовлен Секцией сейсмологии и физики недр Земли Национального геофизического комитета Российской академии наук.

DOI: 10.2205/2015IUGG-RU-IASPEI

Citation: Gliko A.O., A.D. Zavyalov Eds. (2015), National Report for the IASPEI of the IUGG 2011–2014, *Geoinf. Res. Papers*, 3, BS3010, GCRAS Publ., Moscow, 25 pp.
doi: 10.2205/2015IUGG- RU-IASPEI

© 2015 National Geophysical Committee of Russia

Contents

- INTRODUCTION.....4**
- 1. THE STRUCTURE AND RESULTS OF SEISMIC OBSERVATIONS IN RUSSIA4**
- 2. STRONG EARTHQUAKES IN RUSSIA IN 2011-2014 11**
- 3. SEISMOGEOYNAMICS..... 14**
- 4. SEISMIC RISK ASSESSMENT AND MANAGEMENT IN THE RUSSIAN FEDERATION 16**
- 5. PHYSICS OF THE SEISMIC PROCESS AND EARTHQUAKE PREDICTION..... 18**
- 6. INDUCED SEISMICITY AND ITS MONITORING23**

Introduction

This report submitted to the International Association of Seismology and the Physics of the Earth's Interior (IASPEI) of the International Union of Geodesy and Geophysics (IUGG) contains results obtained by Russian geophysicists in 2011-2014. In the report prepared for the XXVI General Assembly of IUGG (Czech Republic, Prague, June 22 – July 2, 2015), the results are briefly outlined of basic research in seismology, geodynamics, in the studies of physics of seismic process and earthquake prediction as well as in some other directions.

The period from 2011 to 2014 was still difficult for Russian geophysics. In spite of the difficulties, Russian scientists participated in practically all conferences of the International Association of Seismology and the Physics of the Earth's Interior (IASPEI), in the General Assemblies, international projects and in a work of international centers. Russian geophysicists obtained a number of fundamentally important new results in the period under review. Many of them are presented in the following sections of this report.

For a number of reasons not all results obtained by Russian scientists on the problems of seismology and physics of the Earth's interior in 2011-2014 are included in the report. At the same time it is hoped that authors may present these results at symposia of IUGG XXVI General Assembly.

1. The structure and results of seismic observations in Russia

1.1. Joint research was conducted with French seismologists concerning the Tohoku earthquake in Japan of 11 March 2011 ($M_w = 9.0$), its two strongest aftershocks, which occurred 30 and 40 minutes after the main shock, and a foreshock, which occurred two days prior to the event. The assessment of the seismic moment and the depth of the source, as well as focal mechanisms for these events are given in **Fig. 1.1**. It should be noted that the magnitude assessment for the strongest aftershock (event 3 on Fig.1.1) exceeds the magnitude value in the Global CMT Catalog by 0.5. (**Institute of Earthquake Prediction Theory and Mathematical Geophysics RAS**)

1.2. The effect of microseism generation during electric sounding sessions using the ERGU 600-2 electric pulse system. It was established that during sessions of electric sounding of the Earth's crust by high powered electric impulses (600 A) a series of microseisms appears in a considerable area around the electric dipole (30*30 km), leading to stress relief in the Earth's crust. Generation of microseisms occurs both during sounding sessions and after them. Microseism generation is caused by forced oscillations in the medium, originating during sounding. Optimal consistent filtration of the

seismic signal allowed to discriminate the response in the seismic field from the impulse charge sequence generated by ERGU 600-2 in the electric dipole. **(Research Station RAS, Bishkek)**

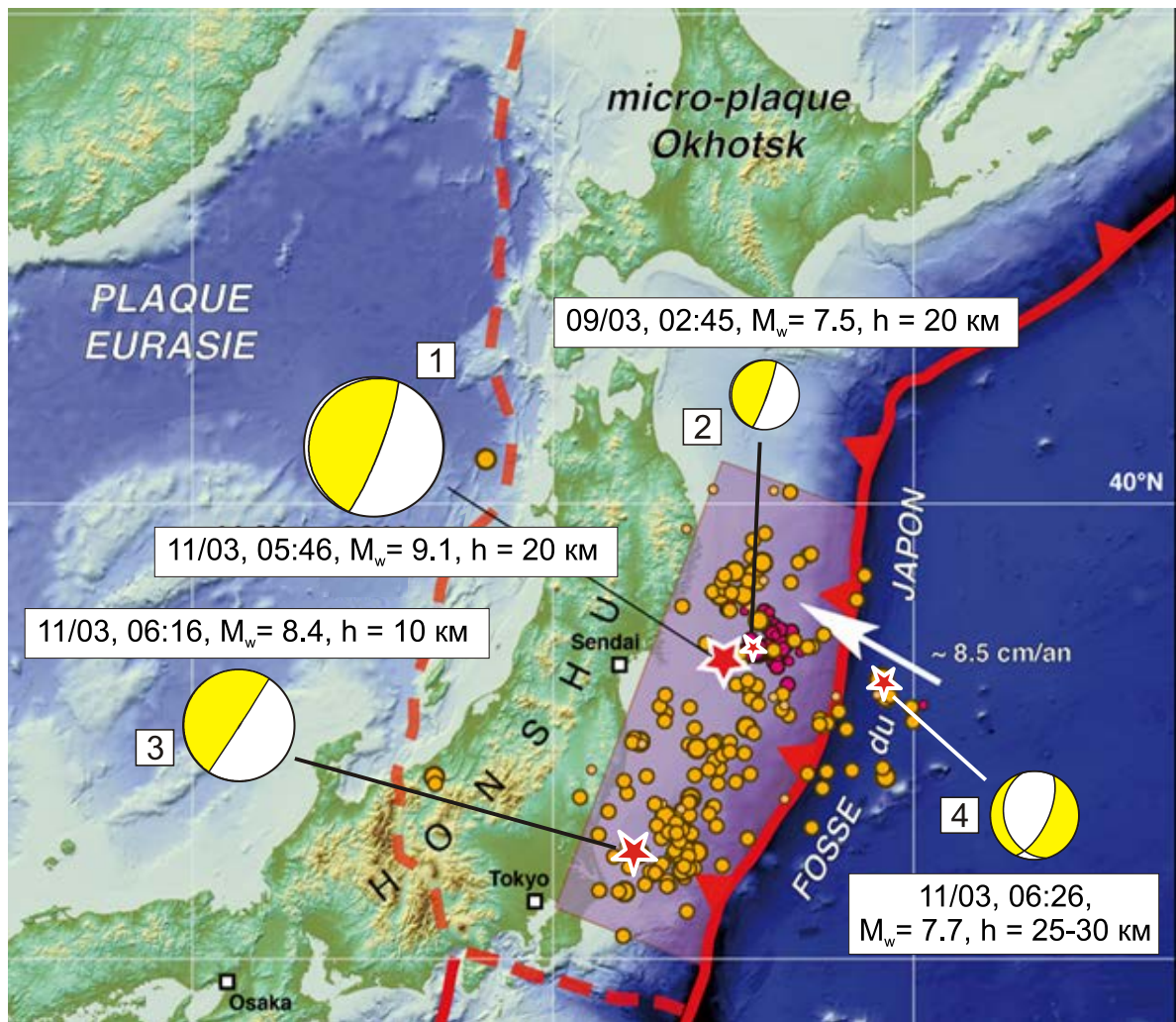


Fig. 1.1. Assessment of source parameters for the main shock (1), the foreshock (2), and two strongest aftershocks (3 and 4) of the Tohoku earthquake. Earthquake epicenters are marked with stars.

1.2. The effect of microseism generation during electric sounding sessions using the ERGU 600-2 electric pulse system. It was established that during sessions of electric sounding of the Earth's crust by high powered electric impulses (600 A) a series of microseisms appears in a considerable area around the electric dipole (30*30 km), leading to stress relief in the Earth's crust. Generation of microseisms occurs both during sounding sessions and after them. Microseism generation is caused by forced oscillations in the medium, originating during sounding. Optimal consistent filtration of the seismic signal allowed to discriminate the response in the seismic field from the impulse charge sequence generated by ERGU 600-2 in the electric dipole. **(Research Station RAS, Bishkek)**

1.3. The source of the Tohoku earthquake of 11 March 2011 ($M_w = 9.0$) was modeled for the spherical Earth based on co-seismic surface shifts, registered by GPS/GLONASS stations at distances up to 2300 km (**Fig. 1.2**). It was determined that the main energy of the earthquake with maximum

movement in the source at 33 m was released in the relatively narrow segment of the seismic fault of 200×96 km. It was demonstrated that usage of far-field GPS data provides an opportunity to promptly assess the parameters of a remote earthquake. (Institute of Applied Mathematics of the Far East Branch of RAS, Institute of Tectonics and Geophysics of the Far East Branch of RAS, Institute of Marine Geology and Geophysics of the Far East Branch of RAS, Institute of Geology and Natural Management of the Far East Branch of RAS in cooperation with the Institute of Seismology and Volcanology of Hokkaido University (Japan) and Kangwon National University (Republic of Korea))

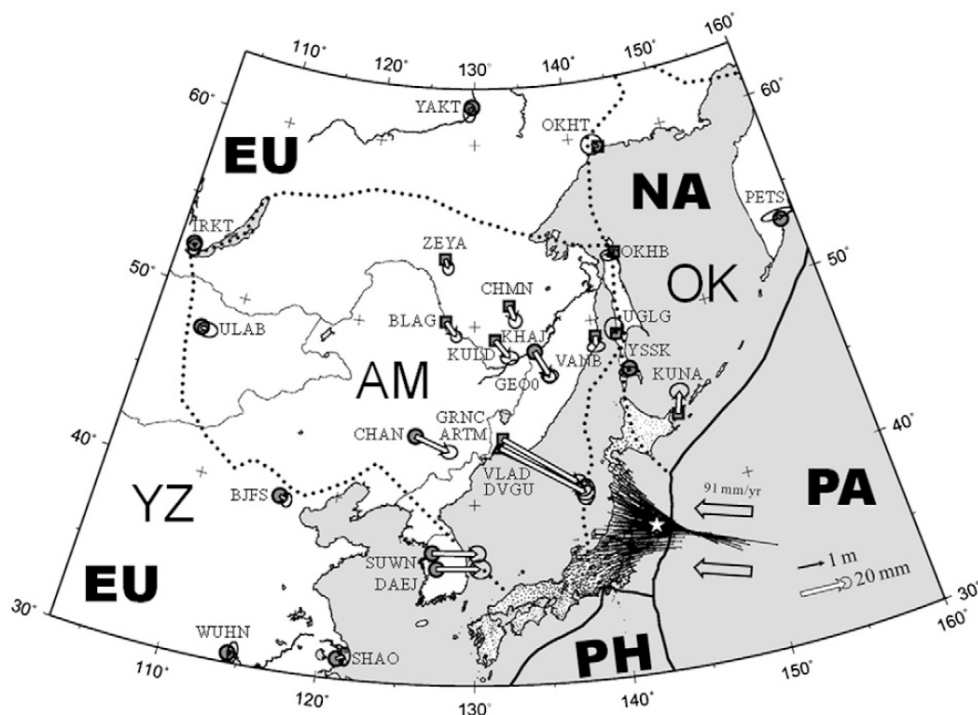


Fig. 1.2. Diagram of horizontal co-seismic surface shifts resulting from the Tohoku earthquake of 11 March 2011, Mw=9.0. Tectonic plates and microplates: EU – Eurasian, NA – North American, PA – Pacific, PH – Philippine, AM – Amurian, OK – Okhotsk, YZ – Yangtze

1.4. A system of recording and processing earthquakes in automatic and dialogue modes operating on a new level of data processing speed was developed. Our own innovative solutions, as well as achievements of major European and American seismological centers, were used in development of this system. Prompt earthquake notification is being dispatched in 1-2 minutes instead of 40 min with the old system. The capacity of the new system allowed to process over twenty two thousand earthquakes in 2012. The system provides an opportunity to move to another level of comprehension of stress with respect to the range of energies and quantity of analyzed earthquakes. (Geophysical Survey, Siberian Branch of RAS, Novosibirsk)

1.5. Reviews were compiled and surveys “Earthquakes in Central Eurasia. 2005-2008” and “Earthquakes in Russia in 2009-2012” were published.

The seismic array in the North Caucasus was developed further: six new seismic stations, fitted with modern digital equipment and located in areas of the highest seismic risk including Greater Sochi, were opened in 2012. In the North Caucasus in general fifty-three stations are fitted with digital equipment, satellite terminals, and other facilities for transmitting data to collection centers for continuous recordings with minimal delay (in a mode close to real time).

The existing central and regional databases of the Geophysical Survey for seismological and geodynamical monitoring, including seismic event catalogs and waveform archives were completed with 2011-2014 data.

The newly created DyfitSettlements system that features a database on populated areas in the Russian Federation and a web-interface for remote access to these data through commonly used browsers. DyfitSettlements is being used within the current version of DyfitWeb for collecting macroseismic data online on the website of the Geophysical Survey of RAS.

The purpose and goals for creating a new information system for seismic data were laid down, the concept of organizing access and storage of seismic data was renewed and the new structure of the unified information system for seismic data for the Kamchatka branch of the Geophysical Survey of RAS was developed.

“The Regional Catalog of Earthquakes in Kamchatka and the Commander Islands” database was registered in the Registry for databases (Certificate #2012620813 of 12.11.2012). **(RAS Geophysical Survey)**

1.6. The earthquake of 11 April 2012 ($M_w = 8.6$), which occurred west of North Sumatra coast was studied to determine the mechanism of its source. A solution was derived from analysis of the amplitude spectrum of Love and Rayleigh waves in the period band 200-300 seconds. A conclusion on sublatitudinal extension of the fault was made **(Institute of Earthquake Prediction Theory and Mathematical Geophysics RAS)**

1.7. A new set of methods and supporting software was created for spectral, spectral-temporal and polarization analysis of wide-band seismic recordings, which allows for different formats of input data and automated batch mode of processing a random number of three-component seismograms, recorded with various equipment and arbitrary frequency responses. Regardless of the type of input data, spectral and other characteristics for velocities, acceleration and other derivative displacements. Software was implemented in the Sakhalin and Kamchatka branches of the Geophysical Survey of RAS. **(Institute of Earthquake Prediction Theory and Mathematical Geophysics RAS)**

1.8. A new technique was developed for combined processing of digital data from matched pairs of seismic and infrasound pulse signals for detecting and localizing seismo-acoustic events, generated by glaciers (**Fig. 1.3**). Application of the new technique allowed to detect and accurately localize seismo-acoustic events, associated with destruction processes in outlet glaciers, on Svalbard (island Spitsbergen). Events occurring on the glacier margins are associated with calving of ice walls on the terminus. In case of tide glaciers or ice margins located at the earth-sea border, this calving lead to iceberg formation. Events occurring away from the margins are connected with crevassing. Seismic infrasound monitoring of ridge-and-valley channel glaciers on the on the north shore of the Is-Fiord Bay on the Island of Spitsbergen was performed in 2012-2013 using new techniques. 242 events were recorded and localized, their connection with the main glacier destruction processes (crevassing, calving) was determined. (**Kola branch of the Geophysical Survey of RAS**)

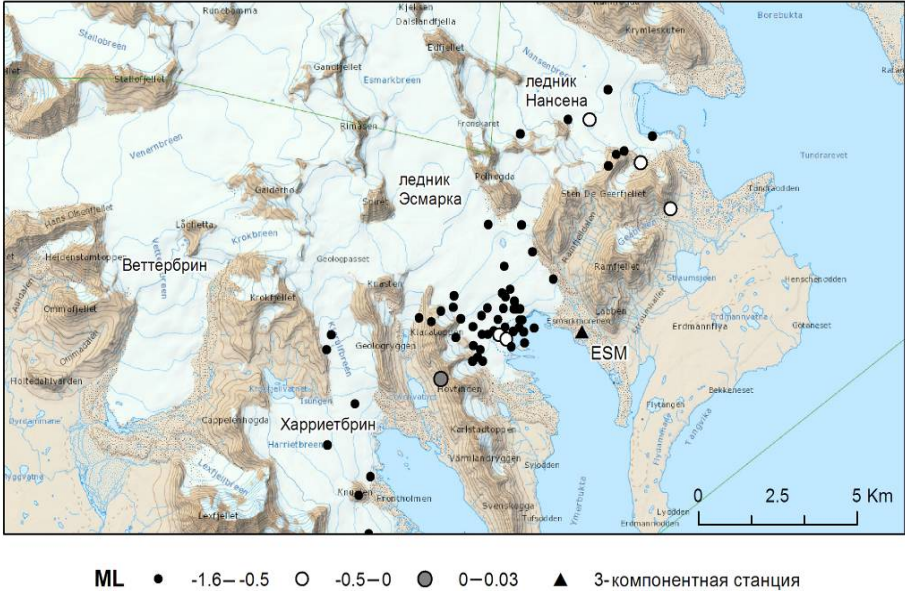


Fig. 1.3. Seismic infrasound events in the glacier area on the north shore of the Is-Fiord Bay from 11 June to 22 Sept 2012.

1.9. A technique of sustainable assessment of the moment magnitude over the range of longitudinal waves M_{wp} of medium and strong earthquakes on wide-band regional seismograms from a high spaced network of stations was developed and tested (**Fig.1.4**). The new technique provides a series of magnitude assessments for a set of frequency bands and determines the choice of the final assessment. The novelty of the technique consists in simultaneous processing of the signal in several frequency ranges; its efficiency was demonstrated on examples of ninety-two earthquakes in the Far East with moment magnitude $M_w=6.5-9.1$, for which a conclusive correlation between M_{wp} and M_w at depths up to 70km and the absence of necessity to introduce a magnitude-dependent correction at this range of depths were shown. The technique is being implemented into the system of seismological observations and tsunami warning in the Russian Far East with the purpose of increasing the speed and accuracy of

assessing tsunamigenic potential of strong earthquakes in an on-line mode and lowering the number of false tsunami alarms. (**Kamchatka branch of the Geophysical Survey of RAS**)

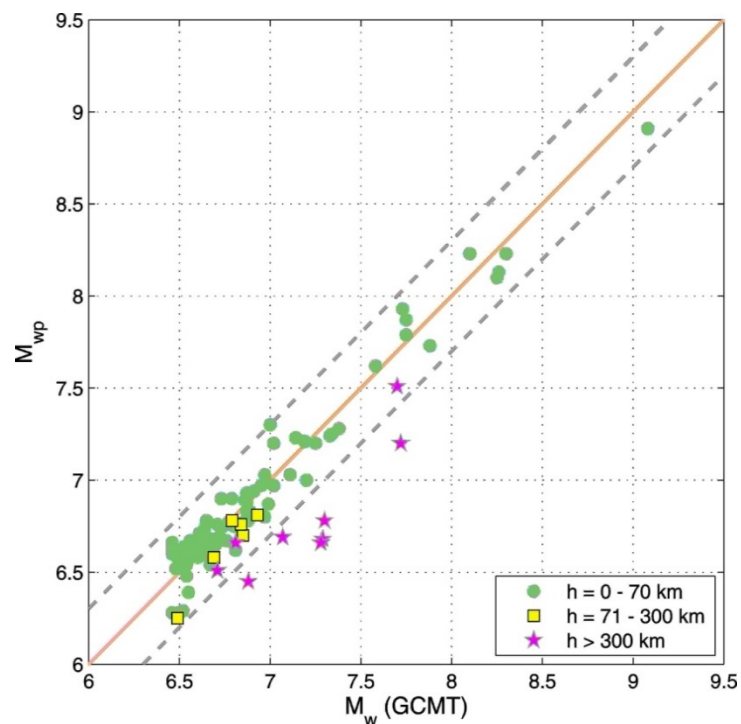


Fig. 1.4. Magnitude M_{wp} as a function of moment magnitude M_w for three hypocenter depth intervals: $h \leq 70$ km, $71 \text{ km} \leq h \leq 300$ km and $h > 300$ km. Dashed lines are ± 0.3 magnitude unit deviations from the perfect trend (solid line).

1.10. A set of investigations was conducted on the Chelyabinsk incident, which allowed to assess the energy of the astronomical object (400-600 kt TNT) according to the infrasound and surface damage (**Fig. 1.5**). It also provided an opportunity to create an energy-yield model based on the light curve and calculate the distribution of air-waves including their impact on the Earth's surface using this model. A satisfactory relationship between the calculated and actual areas of destruction was obtained. It was demonstrated that the energy release was of extended nature and differed significantly from that of a point explosion. (**Institute of Geosphere Dynamics RAS**)

1.11. The Arkhangelsk seismic array was included in the International Federation of Digital Seismograph Networks (FDSN) (<http://www.fdsn.org/networks/>) and assigned seismic code AN. According to the Arkhangelsk array, 50-100 seismic events of various origins occur each month in the Euro-Arctic region (**Fig. 1.6**). Seismic activity on the slope of the continental shelf of the Russian Federation that correlates with anomalous values of the heat flow (Khutorskoy et al., 2009) was detected, which points to ongoing destruction processes on the shelf and requires an in-depth research into the origin and peculiarities of regional seismicity in the area. This research is material for

nonhazardous exploitation of oil and gas field areas. (**Institute of Ecological Problems of the North of the Ural Branch of RAS**)

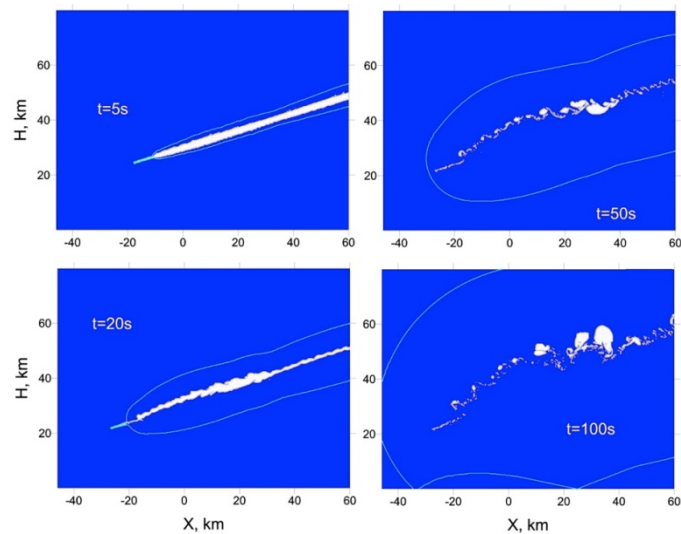


Рис. 1.5. Modeling of the Chelyabinsk meteor entering the atmosphere, generation and distribution of the shock wave (blue line), and the evolution of the trace in the atmosphere. The white trace consists of a mixture of meteor vapors and air, it lingered in the atmosphere for tens of minutes, and thus was clearly seen on multiple photos. X=0 point corresponds to the coordinate of the strongest flare.

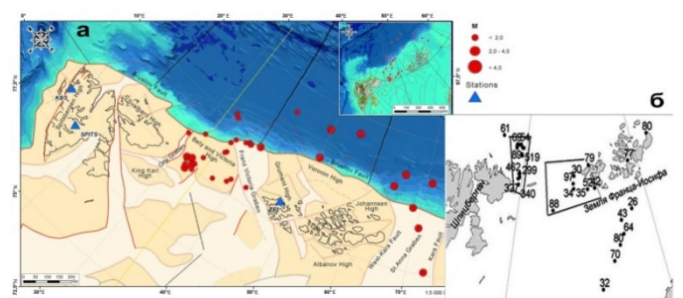
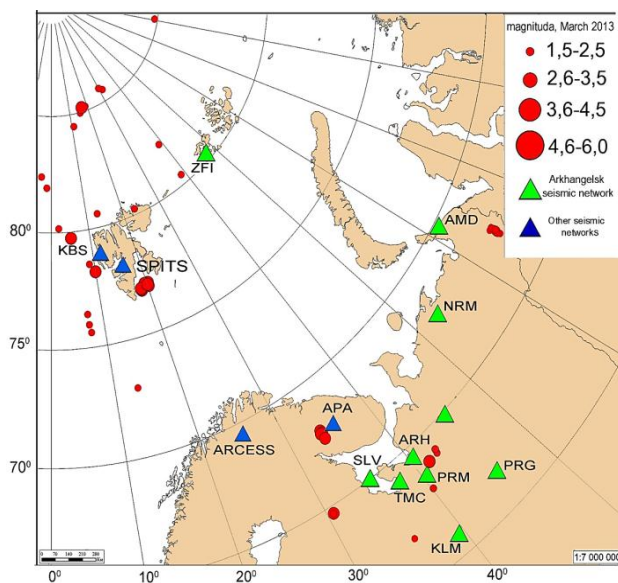


Fig. 1.6. Maps of seismic events recorded with the Arkhangelsk seismic array in March (left) and July (right) 2013.

1.12. A mathematical model was developed and numerical modeling was performed for seismic wave fields in areas of anomalous stress, generated in the interior by tectonic and geodynamic processes. Appearance of anomalously reflected seismic waves was demonstrated using the example of a homogenous elastic half-space. Neglecting this effect can lead to erroneous interpretation of seismic data. (**Institute of Petroleum Geology and Geophysics, Siberian Branch of RAS**)

1.13. As a result of processing new seismic data within the PIRE project, performed in cooperation with Alaskan colleagues, a seismic model beneath the Bezymianny and the Klyuchevskoy volcanoes

was developed. It distinctly shows magmatic dikes in the form of anomalies with increased values of V_p/V_s . It was revealed that dikes beneath the Bezymianny and the Klyuchevskoy volcanoes appear to be independent, at least down to 15 km. The Bezymianny volcano is generally considered to be sustained directly from the mantle, whereas the Klyuchevskoy volcano functions on a system of transitional magma chambers. **(Institute of Petroleum Geology and Geophysics of the Siberian Branch of RAS)**

1.14. A principally new approach to computation of the field of reflection times (times of transit for all source-receiver positions), based on numeric solution of the double root problem instead of multiple eikonal equation solutions. It provides an opportunity to precipitate the solution of the direct kinematic problem for multifold seismic survey observation systems and is projected to be used for solving inverse kinematic problems. **(Institute of Petroleum Geology and Geophysics of the Siberian Branch of RAS)**

1.15. A detailed study of consequences of the South Yakutia earthquake of 20 April 1989, $M=6.6$, was performed. Its magnitude reached 8 in the pleistoseismic zone. It is considered to be among the strongest seismic events in South Yakutia in the last forty-five years. The depth of the shock was 27 km, which significantly exceeds the average values for source depths (10-15 km) for South Yakutia earthquakes in general. Analysis of recurrent shocks after the South Yakutia earthquake over time demonstrates that attenuation of the seismic process occurred exponentially. Displacement type can be determined as oblique-slip fault. Analysis of macroseismic effects of the South Yakutia earthquake and its strong aftershocks on the surface displayed the dependence of their first isoseists on the deep structure of the region. **(Geophysical Survey of the Siberian Branch of RAS, Novosibirsk)**

1.16. Observations involving data from temporary networks of stations helped to establish that ten years after the strong earthquake of 2003 in the Chouya-Kuray zone of the Altai Mountains a tendency towards distribution of the seismic process into areas adjoining the epicentral zone, into the South Chouya, Aygulak, and Kuray ridges. In 2012-2014 an increase of annual release of seismic energy, comparable with the same value during the active phase of the aftershock stage (2004-2005) was recorded. **(Geophysical Survey of the Siberian Branch of RAS, Novosibirsk)**

2. Strong earthquakes in Russia in 2011-2014

2.1. Assessments of source parameters for the deep-focus Sea of Okhotsk earthquake of 24 May 2013, based on integrated data of regional seismic and GPS observations were produced **(Fig. 2.1)**.

Previously, seismic data were the only type to be used for deep-focus earthquakes. Statistical shifts detected at 29 GPS observation points in the Far East and recordings from 28 regional wideband seismic station were independently inverted to seismic moment tensor, which includes the source mechanism and scalar seismic moment M_0 . The divergence in M_0 assessment based on seismic and GPS data does not exceed 14%, which suggests the absence of slow postseismic movements in the source. The source component determined by cubic dilatation or triaxial compression is not detected by either seismic or GPS data. The obtained results are material for comprehending physics of the source of a deep-focus earthquake. (**Kamchatka Branch of the Geophysical Survey of RAS**, see *Abubakirov I.R., Pavlov V.M., Titkov N.N.* The mechanism of the deep-focus Sea of Okhotsk earthquake of 24 May 2013 according to statistical shifts and wide-band seismograms // *Vulkanologiya i seismologiya*, 2014)

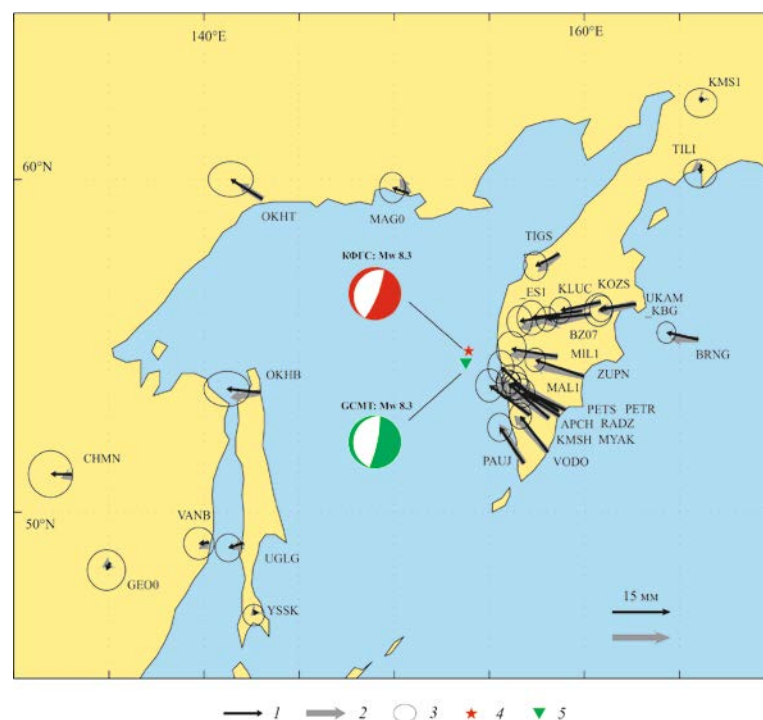


Fig. 2.1. Horizontal components of co-seismic shift jumps from the deep-focus Sea of Okhotsk earthquake of 24 May 2013, $M_w=8.3$ at Far East observation points.

1 – observed shift jumps (vectors tangent to the Earth); 2 – estimated jumps for a model of homogeneous, stratified, spherically symmetrical Earth; 3 – error ellipses, 4 – epicenter according to data from Kamchatka Branch of the Geophysical Survey (KBGS) of RAS; 5– epicenter according to GCMT data. GCMT and KBGS mechanisms are given in stereographic projection of the lower hemisphere of the focal sphere. KBGS mechanism is built on inverting the observed shift jumps.

2.2. GPS/GLONASS stations in the Okhotsk region pioneered in registering co-seismic surface shifts as a result of the Sea of Okhotsk earthquake ($M_w = 8,3$), which happened on 24 May 2013 at the depth of ~ 600 km near the west coast of the Kamchatka Peninsula (**Fig. 2.2**). A dislocation model of a deep-focus earthquake in the elastic half-space factoring in the sphericity and stratification of the Earth (**Fig. 2.2**)

was constructed. There is a low-angle fault in the source with 11° angle west dipping; maximum adjustment is 7 meters; fault width in the downgoing Pacific plate is 50 km. (**Institute of Marine Geology and Geophysics of the Far East Branch of RAS, Institute of Tectonics and Geophysics of the Far East Branch of RAS, Institute of Automation and Control Processes of the Far East Branch of RAS**, see *Steblov G.M., Ekström G., Kogan M.G., et al.* // *Geophysical Research Letters*, 2014, vol. 41, issue 11, pp. 3826–3832. DOI: 10.1002/2014GL060003; *Shestakov N.V., Ohzono M., Takahashi N., Gerasimenko M.D., Bykov V.G. et al.* // *Reports AS*. 2014. v. 457, № 4. pp. 471–476)

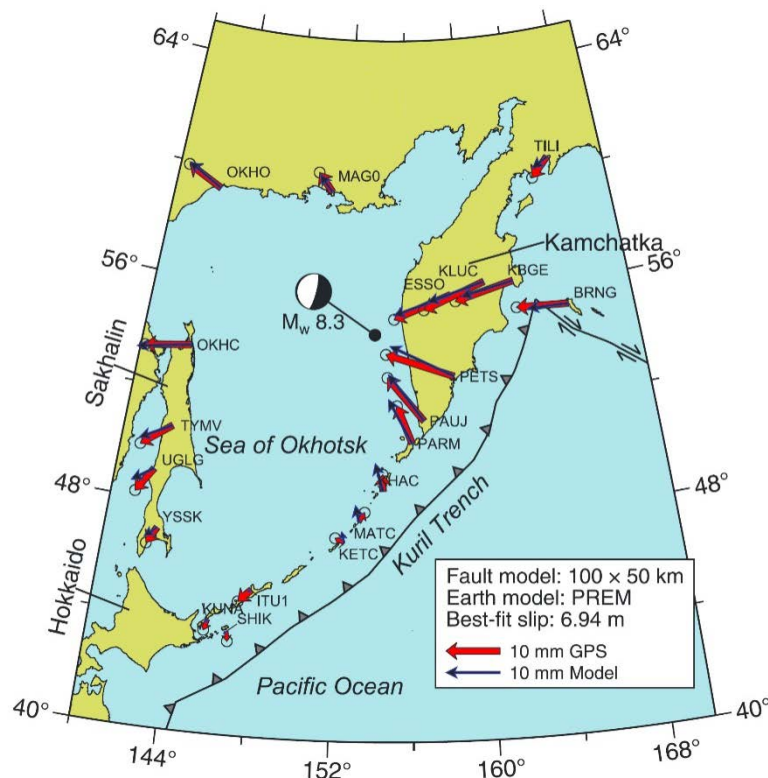


Fig. 2.2. Co-seismic shifts of GPS/GLONASS sites as a result of the deep-focus Sea of Okhotsk earthquake of 24 May 2013, $M_w = 8.3$

2.3. An interpretation was given to the macroseismic effect observed in Moscow, at a distance of approximately 6500 km from the epicenter of the deep-focus earthquake in the Sea of Okhotsk ($M_w=8.3$, $H=609$ km). Based on analysis of records made in the Institute of Physics of the Earth RAS (ultra-long period velocimeter) and at the Moscow and Obninsk seismic stations it was determined that the most probable cause of this effect is the anomalously large amplitude in the group of SSS waves on the vertical component as a result of its superimposition on the surface waves (**Fig. 2.3, 2.4**). (**Institute of Physics of the Earth RAS**, see *Tatevossian R., Kosarev G., Bykova V., Matsievsky S., Ulomov I., Aptekman J.* // *Physics of the Solid Earth*, 2014, № 3, pp. 154–162)

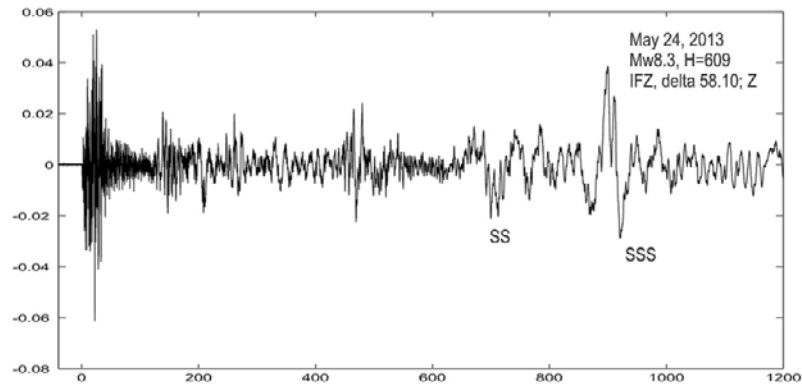


Fig. 2.3. Record of the Sea of Okhotsk earthquake of 2013 ($M_w=8.3$, $H=609\text{km}$), Institute of Physics of the Earth.

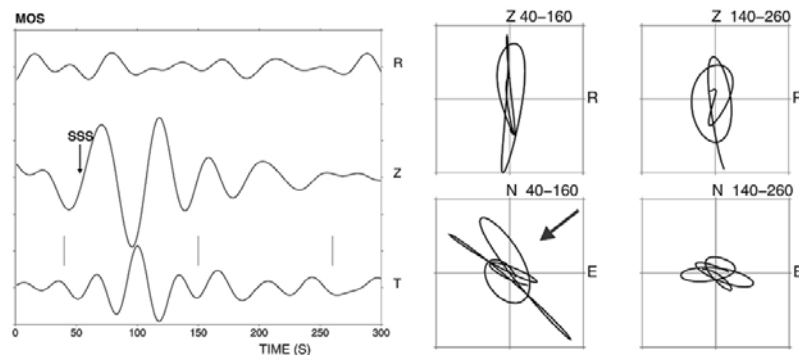


Fig. 2.4. Waveforms (filtered in the band of 30-80 s and rotated) and particle trajectories. SSS-wave arrival is shown according to the IASPEI91 travel-time curve; arrows indicate the direction from the source towards the station. Vertical lines indicate two time windows, for which particle trajectories were calculated (given above the plots).

3. Seismogeodynamics

3.1. A new numeric method (Method of Stress Trajectory Elements, MSTE) for determining tectonic stress fields. Geological and geophysical data on elements of stress trajectories are used in MSTE directly as input data. Based on this method, stress fields that were released in certain island arc areas prior to strong tsunamigenic earthquakes. It was established that the common feature of these fields is decreased value of maximum horizontal tangent stress τ_{\max} in epicenters of future earthquakes. After an earthquake locations of decreased τ_{\max} values shift from their primary position. (Institute of Physics of the Earth RAS)

3.2. A database of geological, geophysical, and seismological data for the Timan-North Urals region. The main methodological aspects of forecasting geodynamically unstable zones based on integrated analysis of geological, geophysical, and seismological data. A model of geodynamically unstable zones in the region was built using GIS technologies. This model served as basis for a forecast map of maximum magnitudes of earthquakes in the Timan-North Urals region. Five geodynamically unstable

zones were detected: Sysolsky, Mezensky, North Timan, Izhemsky, and Upper Pechorsky (**Komi Institute of Geology of the Ural Branch of RAS**).

3.3. The parameters of splitting S-waves from deep-focus earthquakes (160-550 km) in the back-arc area of the Kuril Island arc (Sakhalin and Hokkaido). Symmetry of the geological medium within an orthorhombic and a transversally isotropic model (**Fig. 3.1**). Beneath the Sea of Japan the distribution of the fast S-wave azimuth corresponds to the geometry of the downgoing plate; beneath the Sea of Okhotsk and Sakhalin it coincides with the intermediate axial inclination. It is posited that the mantle plume is oriented along the intermediate axis, which corresponds to the shear direction under the conditions of an increased heat flow. The minimum degree of anisotropy (1–2.5%) was detected beneath the Island of Sakhalin, and the maximum (3–5%) – beneath the Sea of Japan. (**Institute of Tectonics and Geophysics of the Far East Branch of RAS**)

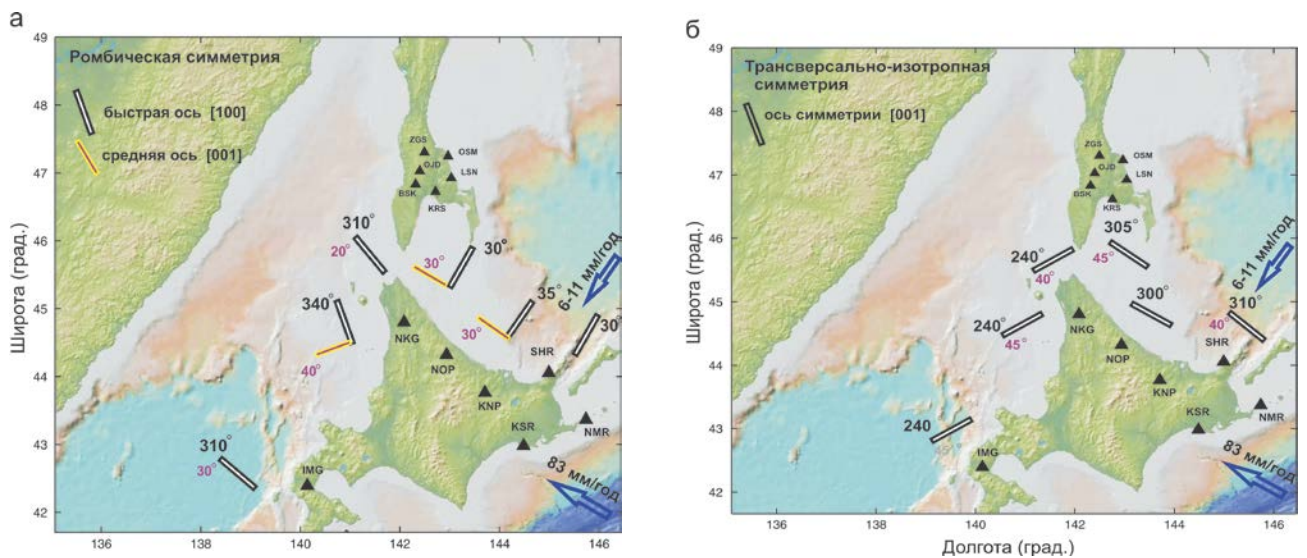


Fig. 3.1. Orientation of the fast [100] and intermediate axes (a) of orthorhombic symmetry and the axis [001] of transversally isotropic symmetry of the medium beneath South Sakhalin and Hokkaido. Arrows mark the direction and velocity of the Pacific plate movement. Triangles show the location of stations. Azimuth (black font) and tilt angle (purple font) of the symmetry axis against the horizontal surface are given in numbers.

3.4. A novel tectonophysical concept of the seismic process and a model of the continental seismic zone in the metastable fault block lithosphere medium were developed. The distortion of its balance and initiation of the seismic process are mainly caused by strain waves. Their front exercises a dynamic impact on the whole system of blocks, selectively activating interblock faults, whose movements generate seismic events. For certain seismic zones in Central Asia time-source generation location regressional dependencies, which allow to perform medium-term earthquake predictions, were established. (**Institute of the Earth's Crust of the Siberian Branch of RAS**)

4. Seismic Risk Assessment and Management in the Russian Federation

4.1. The Specialized Catalog of Earthquakes in North Eurasia (from ancient times to 2010) was supplemented with new data. The software which was used to build general seismic zoning maps (GSZ-97) was improved. The input database was completely updated. The technique for computation and mapping seismic influences was considerably updated by substituting the rectangular survey grid with a finer and truer for the spherical Earth's surface triangular one covering the whole area of mapping. Models of general seismic zoning maps (GSZ-2012) for frequencies of 500, 1000, 2500, 5000, and 10 000 years were made. **(Institute of Physics of the Earth RAS)**

4.2. Patterns of fluctuations of seismic impact parameters depending on the depth of foundations of buildings and structures were detected. Complex multifactorial influence of the structure, physical, mechanical, and seismic properties of the soil body on the characteristics of seismic impacts in the three-dimensional space of the geological medium were established. Novel principles of compiling geological-geophysical models of the medium for depths of 100 m and deeper were developed. The methodology of instrumental geological-geophysical and seismological technology investigations, material to performing three-dimensional seismic microzoning, was substantiated. In practice, this allows to predict characteristics of seismic impacts from earthquakes on embedded and underground structures, to lower social and economic seismic risk, and to provide a higher level of safety for population. **(Institute of Environmental Geoscience RAS)**

4.3. Experimental research in registering parameters of seismic fields in areas with sites of critical facilities provided an opportunity to assess the level of activation of regional seismicity. It was demonstrated that the usage of new techniques and equipment for monitoring the dynamics of seismotectonic processes permits to specify, record, and assess seismic risk in areas with sites of critical facilities, first and foremost nuclear power plants (NPP). Monitoring of geodynamic processes and seismic risk assessment for areas with all NPPs in the Russian Federation were performed. The ensuing results helped increase safe operation of NPP units due to a considerable rise in integration and accuracy of substantiation of seismic safety for NPP site locations. They can be used as input materials in approving project designs. **(Institute of Physics of the Earth RAS)**

4.4. A new approach to seismic risk assessment based on using catalogs of observed and modeled seismicity and computation of peak acceleration for each event to create stochastic catalogs of earthquakes with significant cumulative time span. The approach was applied to the Tibet-Himalaya region. Modeled seismicity was obtained from modeling the dynamics of the block structure of the

region. Comparison of the resulting seismic risk assessment with GSHAP results (**Fig. 4.1**) manifests its higher accuracy in predicting peak acceleration (e.g. in Sichuan, where a strong earthquake occurred in 2008). (**Institute of Earthquake Prediction Theory and Mathematical Geophysics RAS**)

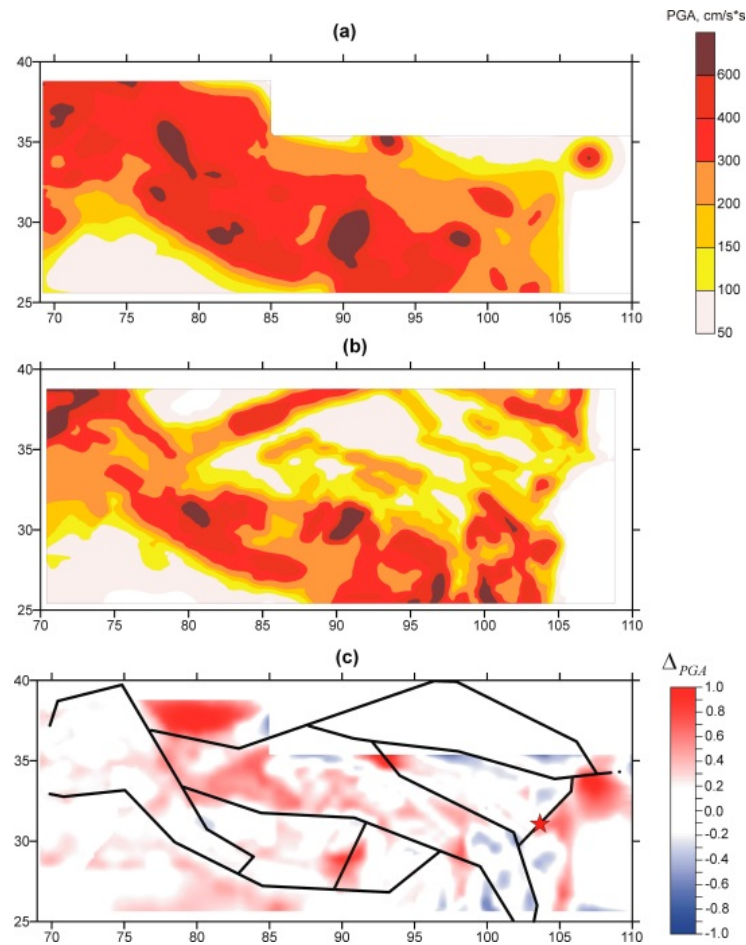


Fig. 4.1. Seismic risk maps for the Tibet-Himalaya region (peak ground accelerations (PGA) for 475-year frequencies): (a) proposed approach, (b) according to GSHAP, (c) difference between the two assessments. Black lines on (c) mark the system of main blocks in the region, the red star marks the epicenter of the 2008 Sichuan earthquake.

4.5. An effect of amplification of ground oscillations due to their resonance re-emission by buildings and structures. In areas built-up with multi-story buildings at certain frequencies ground oscillation amplitudes can increase steeply, which is connected with resonance phenomena in structures standing on their surface. The increment of seismic intensity due to this effect can exceed manifold the increment connected with local geological conditions, which is important to take into account while performing seismic microzoning. (**Institute of Petroleum Geology and Geophysics of the Siberian Branch of RAS, Geophysical Survey of the Siberian Branch of RAS**).

4.6. Models of general seismic zoning (GSZ-2014) maps of the Russian Federation intended for increasing efficacy of anti-seismic construction of objects from different safety categories (A, B, C)

and for lowering social and economic damage from strong earthquakes. An updated catalog of seismic events supplemented with data for the last twenty years and a combined nonlinear model of seismic regime were used to create GSZ-2014 maps. The model is similar to the model developed for compilation of standard GSZ-97 maps. **(Institute of Physics of the Earth RAS)**

4.7. A new seismic scale based on the improved technique for computing synthetic accelerograms and spectral characteristics of seismic impacts was developed. First public discussions were held on the “Seismic intensity scale” Federal Standard R project. **(Institute of Physics of the Earth RAS)**

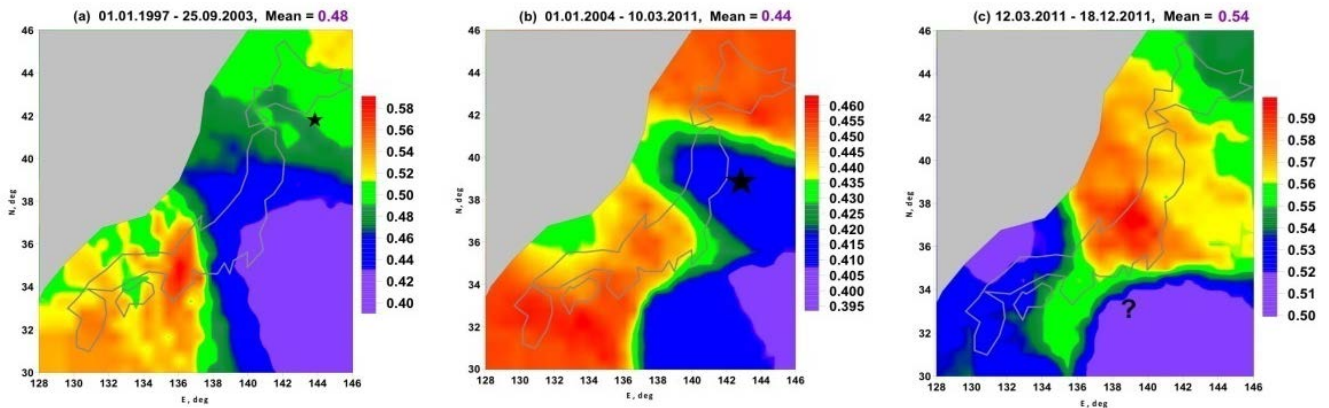
5. Physics of the seismic process and earthquake prediction

5.1. A new technique was developed for dynamic assessment of seismic risk based on analysis of low-frequency seismic noise from a network of stations. This analysis permits to predict the location of a future natural disaster as an area of decreased values of multi-fractal singularity spectrum support width. One example of applying the developed technique is the long-term prediction of the Japan earthquake of March 11, 2011 (**Fig. 5.1**). This prediction was published and presented at Russian and international conferences well before the event, first in 2008 with only magnitude assessment, then in 2010 with timeframe assessment. **(Institute of Physics of the Earth RAS)**

5.2. Seismic observation data revealed space-time variations of mechanical characteristics of the Earth’s crust, localized in fault zones in both seismic and aseismic regions. A double alteration of rigidity in fault zones of the Eastern European platform with a number of distinct period was detected (**Fig. 5.2**). The effect of rigidity alteration in fault zones at various stages of the seismic cycle was quantitatively described for the first time and it was established that shear rigidity of the fault decreases drastically during the final stage of earthquake preparation. The obtained results serve as basis for developing new active and passive seismic monitoring techniques for regions with varying tectonic conditions. **(Institute of Geosphere Dynamics RAS, see Kocharyan G.G., Ostapchuk A.A. Rigidity alteration of the fault zone during the seismic cycle // Reports AS, 2011, v. 441, №3, p. 384-387)**

5.3. Patterns of subsurface temperature variations during earthquake preparation and occurrence were detected. The temperature “signal” correlating with a seismic event is most observable at the depth of 240 m; it reflects fluid exchange between the deformed layers. The reaction of the temperature field to earthquake preparation and occurrence is persistent for seismic events with $M \geq 2.5 \lg R$, where R is

epicenter distance in km, This reaction manifests itself as a consistent decrease of temperature before an earthquake and its steep increase after it. (Institute of Geophysics of the Ural Branch of RAS)



Beginning of 1997 – 25 Sept. 2003: area of the future seismic disaster is characterized by relatively low values of $\Delta\alpha$. It is not split into the northern and southern sections yet.

Beginning of 2004 – 10 March 2011: area of the future seismic disaster is characterized by relatively low values of $\Delta\alpha$. The previous single area of low values of $\Delta\alpha$ split into the northern and southern sections.

12 March – 18 Dec. 2011: northern section of low values of $\Delta\alpha$ transformed into the area of the Tohoku earthquake of 11 March 2011, $M=9.0$, whereas the southern section is still characterized by relatively low values of $\Delta\alpha$ and constitutes a risk as an area of a future earthquake with $M>8.5$. Magnitude assessment results from the relative equality of the northern and southern sections of low values of $\Delta\alpha$.

Fig. 5.1. Maps of spatial distribution of multi-fractal singularity spectrum support width $\Delta\alpha$. Areas of relatively low values of $\Delta\alpha$ (blue and purple areas) show regions of synchronization and high risk.

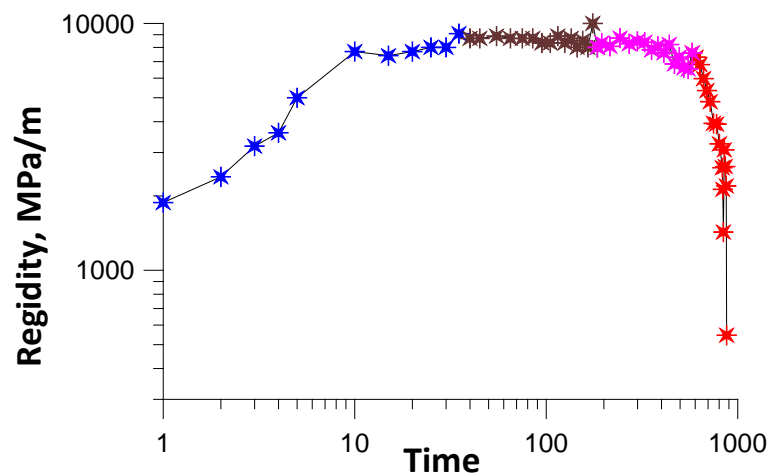


Fig. 5.2. Rigidity alterations of the fault line during the dynamic instability preparation cycle.

5.4. A model of seismic regime as an assemblage of randomly developing episodes of avalanche-like relaxation, occurring at a set of metastable subsystems, was applied to the South Sakhalin region. The values of space changeability of the scaling parameter and of temporal changeability of the parameter of metastability were calculated. The anomalous increase of the parameter of metastability was found in connection with the Gornozavodsk (2006) and Nevelsk (2007) earthquakes (**Fig. 5.3**). Since 2010 high values of this parameter occur south of the Poyasok Isthmus (latitude 48.0°N), which gives ground to consider this region to be an area of preparation of another strong earthquake. (**Institute of Marine Geology and Geophysics of the Far East Branch of RAS**)

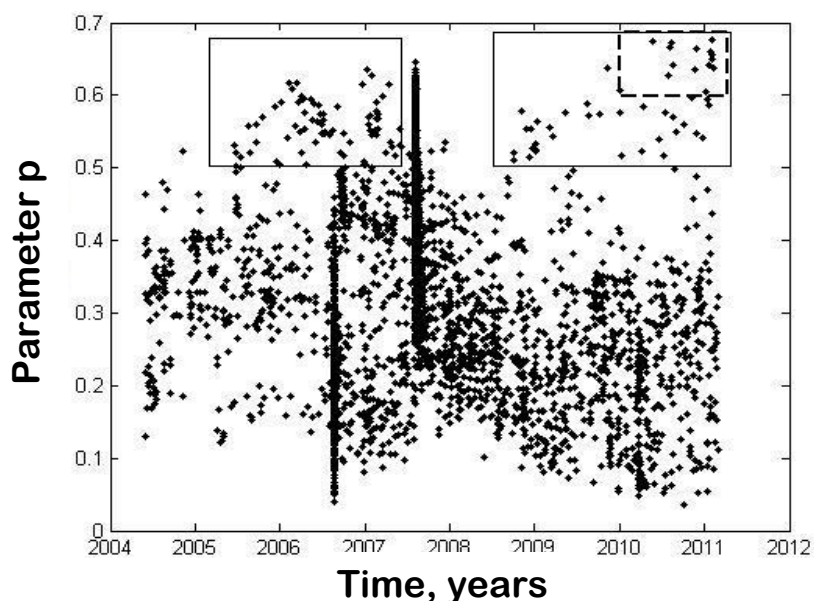


Fig. 5.3. Temporal changeability of the parameter of metastability (p) in the South Sakhalin region for 2004-2011, according to event catalog with $M \geq 2.0$. Rectangles mark groups of events with anomalously high values of p , detected before and after the Nevelsk earthquake.

5.5. Systematization of materials on predicting strong earthquakes in the Kamchatka region in 2012 was performed. The state of seismicity in the Kamchatka region in 2012 was analyzed. Assessments of a range of parameters, including the level of seismicity according to the statistical assessment of the level of seismicity (SOUS'09) scale, the slope in the recurrence relation, seismic activity, etc. were obtained. A search for anomalies of seismic regime using RTL and Z-test prediction methods was conducted in online mode. Retrospective analysis of seismic data allowed to detect an anomaly in the seismic regime prior to the beginning of the Tolbachik fissure eruption in 2012. The anomaly is revealed in the parameters of low energy level seismicity and consists of a statistically significant seismic activation. The duration of the anomaly (from the appearance of a possibility to identify it in online mode) is at least 3 months. (**Geophysical Survey of RAS**)

5.6. GIS technologies were used to recognize potential locations of strong ($M \geq 7.0$) earthquakes in the Black Sea – Caspian region. The result is given on **Fig. 5.4**. It correlates well with the distribution of

5.9. The reaction of earthquakes in Kamchatka with minimum energy class $K \geq 8.5$ to two hundred and fourteen strong earthquakes with $M \geq 7.5$ and forty earthquakes with $M \geq 8$ in the years 1963-2012, distances from sources of strong earthquakes to the center of the seismic zone in Kamchatka being at 600-16000 km. It was determined that remote earthquakes caused an increase of seismic activity, at least in cases where relative dynamic deformations induced by surface waves exceeded 10^{-6} . This corresponded to additional stresses of 10^{-2} MPa, accelerations over 0.1 cm/s^2 , and surface wave periods of ~ 20 s. The response to remote earthquakes increased gradually during several days. The sensitivity of the response differed with time, which manifested itself in intervals of several decades. **(Institute of Physics of the Earth RAS)**

5.10. Two large seismic activations in the Mid-Baikal area, of 2008 and 2011, were studied to analyze the peculiarities of the seismic regime and the stress-strain state of the Earth's crust. In the vicinity of the south-east edge of the lake, in the epicentral zone of the first sequence, new submeridional and sublatitudinal destruction lines were revealed, which previously hadn't been detected using geological and geophysical data. A study of the second sequence of earthquakes confined to offshoots of the Ulan-Burgasy ridge brought about facts indicative of a continuing process of crustal tension structure development south-east of the rift. **(Institute of Geology of the Siberian Branch of RAS).**

5.11. A study of records of wideband seismic stations revealed effects of generation of coherent oscillations on the local and global scale following earthquakes with $M \geq 7$. The effects manifest themselves most distinctly in the range of periods from 5 to 10 min. Coherence can be traced no earlier than 3.1 hours after an earthquake and persists for one to several days, depending on the magnitude. In the $M \geq 7$ earthquakes that occurred between January 1, 2000 and March 11, 2011 on the planet a statistically significant increase of the quantity of subsequent shocks within three days was detected. This coincides with periods of coherent oscillations and can be indicative of the influence of coherent oscillations on potential earthquake sources in a metastable state. The results also show a possible cause of long-range earthquake interaction. Thus, a new mechanism of long-range earthquake interaction is suggested, which can be applied to improving techniques of predicting this type of natural disasters. **(Institute of Physics of the Earth RAS)**

5.12. A new method of combining radically different types of earthquake prediction was developed. It allows to dynamically assess the varying seismic risk factoring in the long-term variations of geophysical fields. The method is applicable to combining predictions of the two following types: 1. assessment of earthquake probability in a given space-time point; 2. detection of areas and intervals of higher (but undetermined) probability. The first type also includes long-term assessments of seismic risk; the second includes all earthquake precursors. Reliability of the combined prediction method

exceeds reliability of each of the initial prediction techniques. **(Institute of Earthquake Prediction Theory and Mathematical Geophysics RAS)**

5.13. The state and energy potential of seismicity at different levels of the lithosphere of the Baikal region was assessed. Experimental studies of the fluid regime and seismic sources revealed that generation and location of riftogenesis attractor structures in the Baikal rift system correlate with the dynamic and energy of fluid systems and zones of deep faults. **(Institute of the Earth's Crust, Siberian Branch RAS)**

6. Induced seismicity and its monitoring

6.1. Analysis of many years of seismic monitoring data yielded a set of main factors influencing seismicity in potassium mines of the Verkhnekamsk potassium salt deposit: quantity of exhausted strata, lithologic type of mined strata, their physical and mechanical properties, presence of stowing, time after mining. **(Mining Institute of the Ural Branch of RAS, in cooperation with the Mining Institute of the Siberian Branch of RAS et al.)**

6.2. Instrumental observation data revealed that seismic oscillations generated by industrial explosions play an important part in the evolution of deformation processes on the East-European Platform and its margins (**Fig. 6.1**). Cumulative seismic energy of explosions exceeds the seismic energy, emitted per year by tectonic earthquakes in the region, by two orders. The effect of accumulation of permanent deformations is significant for those areas of rock massifs, where there is a possibility for instabilities in open-pit walls, slopes, excavations, critical areas of engineering structures. This should be taken into account in compiling new maps of seismic zoning. **(Institute of Geosphere Dynamics RAS)**

6.3. An integrated method of seismic monitoring of strategic sites (nuclear power plants) using small-aperture seismic arrays was developed and tested (**Fig. 6.2**). The method includes computation of small-aperture seismic array configurations, algorithms for seismic signal processing, determining source parameters, determining and monitoring stability of seismic regime parameters. The method was applied in situ on sites of the Leningrad and Nizhny Novgorod nuclear power plants. **(Institute of Geosphere Dynamics RAS)**

6.4. The macroseismic field equation describing the Ural region was revised. The revised equation $I=1.5M-2.3\lg(R)+0.3$, where I is seismic intensity, M – magnitude, R – hypocentral distance, assesses seismic effect at relatively short epicenter distances (0.5-20 km) for shallow sources, which are typical for human-induced seismicity in mining regions. **(Mining Institute of the Ural Branch of RAS)**

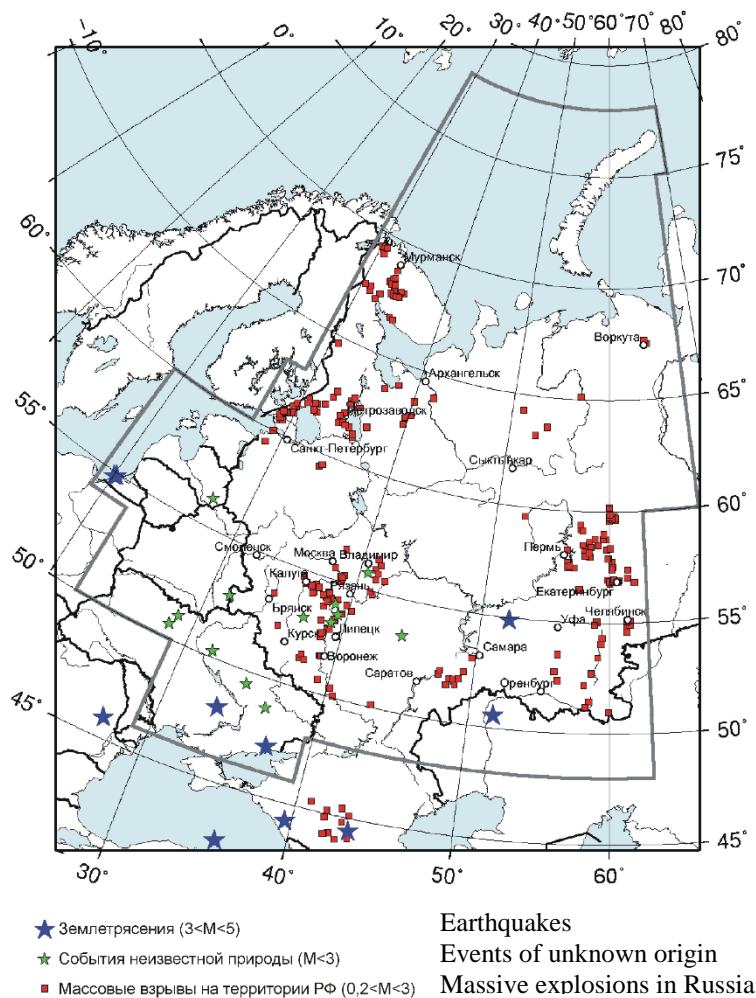


Fig. 6.1. Distribution of epicenters and explosions in the East-European Platform for 2004-2010.

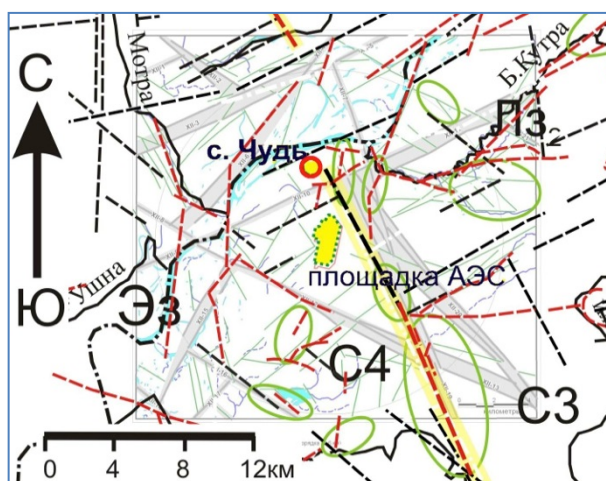


Fig. 6.2. Location of the Monakovo small-aperture seismic array on the outskirts of Chud village (Nizhegorodskaya oblast, Navashinsky region). The location of the array is marked by a red circle showing the area where equipment was installed.

6.5. Experiments proved that induced seismicity in the Kuznetsk Basin is considerably more active than natural seismicity. The most intensive seismic events are stable over time and connected with

mining in rather than the tectonics of the region. (**Geophysical Survey of the Siberian Branch of RAS**)

6.6. A detailed study of the strongest human-induced earthquake on Earth with $M=6.1$, which occurred on June 18, 2013 in the Kuznetsk Basin (Bachatsky open cast area) was conducted using permanent and temporary networks of stations. Macroseismic investigations of the territory show that populated areas in the immediate vicinity of the epicenter endured tremor rate 7, some buildings were destroyed. The 5 rate zone included several towns and the earthquake was felt even outside the Kemerovo region. A temporary network of stations, installed a day after the main event in the Bachatsky open cast area registered a strong aftershock process. The strongest aftershocks had local magnitude over 4. Thirty to fifty earthquakes occurred daily for the first several days after the main event, in a few months the level of activity dropped to a dozen earthquakes per day. (**Geophysical Survey of the Siberian Branch of RAS, Novosibirsk**)